Continuum modeling of van der Waals interactions between carbon nanotube walls

W.B. Lu[1], B. Liu[1a)], J. Wu[1], J. Xiao[2], K.C. Hwang[1], S. Y. Fu[3], Y. Huang[2,4 a)]

[1]FML, Department of Engineering Mechanics, Tsinghua University, Beijing 100084, People's Republic of China,

[2]Department of Mechanical Engineering, Northwestern University, Evanston, Illinois 61801, USA,

[3]Technical Inst. of Physics & Chemistry, Chinese Academy of Sciences, Beijing 100190, People's Republic of China,

[4]Department of Civil & Environmental Eng., Northwestern University, Evanston, Illinois 61801, USA,

ABSTRACT

Prior continuum models of van der Waals force between carbon nanotube walls assume that the pressures be either the same on the walls, or inversely proportional to wall radius. A new continuum model is obtained analytically from the Lennard-Jones potential for van der Waals force, without the above assumptions. Buckling of a double-wall carbon nanotube under external pressure is studied, and the critical buckling pressure is much smaller than those models involving the above assumptions.

[a)] Authors to whom correspondence should be addressed. Electrical addresses: y-huang@northwestern.edu and liubin@tsinghua.edu.cn

In order to overcome limitations of atomistic simulations, continuum models have been developed for carbon nanotubes (CNT), such as the linear elastic shell theory[1,2], finite-deformation membrane theory[3] and shell theory[4] based on interatomic potentials. For multi-wall CNTs, the interaction between walls is governed by the van der Waals force, which is characterized by the Lennard-Jones 6-12 potential, $V(d) = 4\varepsilon \left[(\sigma/d)^{12} - (\sigma/d)^{6} \right]$, where d is the distance between a pair of atoms, and $\sigma = 0.3415nm$ and $\varepsilon = 0.00239ev$ for carbon[5]. Its derivative gives the force between two atoms, $F = V'(d)$ (positive for attractive force).

There are two types of continuum models to represent the van der Waals force between CNT walls. One assumes the pressure to be the same, $p_{in} = p_{out}$, between two adjacent CNT walls[6], where p_{in} and p_{out} are pressures on the inner and outer walls. The other assumes the pressure to be inversely proportional to the wall radius[7,8], i.e., $p_{in} R_{in} = p_{out} R_{out}$, where R_{in} and R_{out} are the inner and outer wall radii (Fig. 1).

The purpose of this letter is to avoid the above assumptions and obtain the pressures on inner and outer walls analytically from the Lennard-Jones 6-12 potential. Such analytical expressions will be useful in the continuum modeling of multi-wall CNTs and their composite materials. Analytical expressions are also obtained for the effective pressures on the inner and outer walls of electrically charged double-wall CNTs.

Cylindrical coordinates (R, θ, z) are used for the double-wall CNT with the inner and outer radii R_{in} and R_{out} shown in Fig. 1. Without losing generality, the distance between an atom on the inner wall ($R_{in}, 0, 0$) and an atom on the outer wall (R_{out}, θ, z) is

$d = \sqrt{R_{in}^2 + R_{out}^2 - 2R_{in}R_{out}\cos\theta + z^2}$. The forces between two atoms are equal and opposite, and

are obtained from the Lennard-Jones potential as $F = V'(d)$ (Fig. 1). Their projections along

the normal direction give the normal forces as $F_R^{in} = F(R_{out}\cos\theta - R_{in})/d$ and

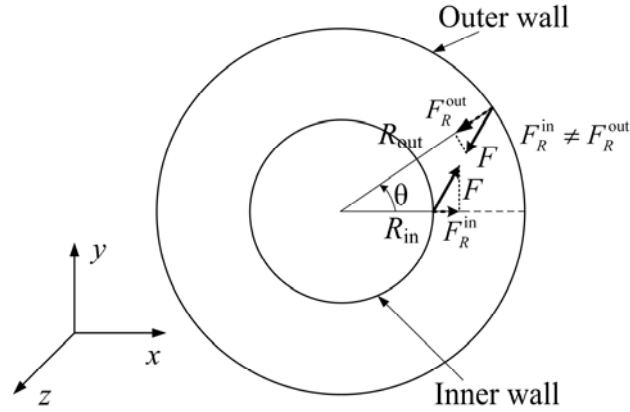$F_R^{out} = F(R_{out} - R_{in}\cos\theta)/d$, which are not equal anymore (Fig. 1).

Figure 1. A schematic diagram of double-wall carbon nanotube

The carbon atoms on each wall are represented by their area density $\rho_c = 4/(3\sqrt{3}l_0^2)$

such that the number of carbon atoms is $\rho_c dA$ over the area dA, where l_0 is the equilibrium bond

length (of graphene). This accurately represents the average behavior of van der Waals

interactions between atoms from adjacent CNT walls[9]. For an infinitesimal area dA_{in} on the

inner wall, the net force in the normal direction is

$\rho_c dA_{in}\int_A F_R^{in}\rho_c dA_c = \rho_c^2 dA_{in}\int_{-\infty}^{\infty} dz\int_0^{2\pi} F(R_{out}\cos\theta - R_{in})d^{-1}R_{out}d\theta$, which gives the pressure on the

inner wall as $p_{in} = -\rho_c^2 R_{out}\int_{-\infty}^{\infty} dz\int_0^{2\pi} F(R_{out}\cos\theta - R_{in})d^{-1}d\theta$ (positive for compression).

Similarly, the pressure on the outer wall is $p_{out} = -\rho_c^2 R_{in}\int_{-\infty}^{\infty} dz\int_0^{2\pi} F(R_{out} - R_{in}\cos\theta)d^{-1}d\theta$.

For the Lennard-Jones 6-12 potential, the above pressures are obtained analytically as

3

$$p_{in} = \frac{3\pi\varepsilon\sigma\rho_c^2 R_{out}}{32 R_{in}} \left[\begin{array}{c} 231\left(\dfrac{\sigma}{R_{in}+R_{out}}\right)^{11}\left(\dfrac{R_{out}-R_{in}}{R_{out}+R_{in}}E_{13}-E_{11}\right) \\[3mm] -160\left(\dfrac{\sigma}{R_{in}+R_{out}}\right)^{5}\left(\dfrac{R_{out}-R_{in}}{R_{out}+R_{in}}E_{7}-E_{5}\right) \end{array} \right], \qquad (1)$$

and

$$p_{out} = \frac{3\pi\varepsilon\sigma\rho_c^2 R_{in}}{32 R_{out}} \left[\begin{array}{c} 231\left(\dfrac{\sigma}{R_{in}+R_{out}}\right)^{11}\left(\dfrac{R_{out}-R_{in}}{R_{out}+R_{in}}E_{13}+E_{11}\right) \\[3mm] -160\left(\dfrac{\sigma}{R_{in}+R_{out}}\right)^{5}\left(\dfrac{R_{out}-R_{in}}{R_{out}+R_{in}}E_{7}+E_{5}\right) \end{array} \right], \qquad (2)$$

where $E_m = \int_0^{\pi/2}\left(1-k^2\sin^2\theta\right)^{-m/2}d\theta$, and $k^2 = 4R_{in}R_{out}/\left(R_{in}+R_{out}\right)^2$; E_m satisfies the recurring

relation $(m-2)\left(1-k^2\right)E_m = (m-3)\left(2-k^2\right)E_{m-2}-(m-4)E_{m-4}$, and

$E_1 = K(k) = \int_0^{\pi/2}\left(1-k^2\sin^2\theta\right)^{-1/2}d\theta$ and $E_{-1} = E(k) = \int_0^{\pi/2}\sqrt{1-k^2\sin^2\theta}\,d\theta$ are the complete
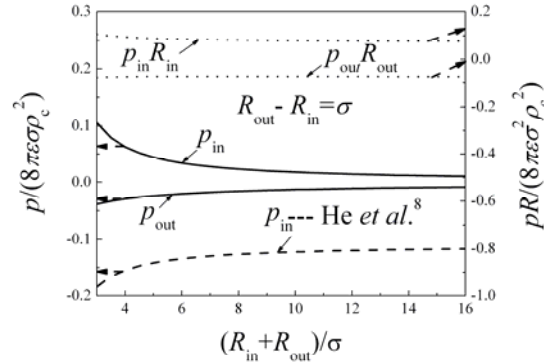
elliptic integrals of 1st and 2nd kind, respectively.

Figure 2.   The normalized pressure, and pressure multiplied by the wall radius R, on the inner and outer walls of a double-wall CNT versus the normalized sum of inner and outer wall radii.   Results of Ref. 8 are also shown for comparison.

Figure 2 shows the normalized pressure, $p/\left(8\pi\varepsilon\sigma\rho_c^2\right)$, versus normalized radius,

$\left(R_{in}+R_{out}\right)/\sigma$, for the inter-wall spacing $R_{out}-R_{in}=\sigma$, which is the equilibrium spacing due to

van der Waals force between graphenes[9]. It is observed that p_{in} and p_{out} have different signs, and therefore $p_{in} \neq p_{out}$. The result of He $et\ al.$[8], $p_{in} = -\rho_c^2 \int_{-\infty}^{\infty} dz \int_0^{2\pi} F R_{out} d\theta$, also shown in Fig. 2, is (in absolute value) much larger than Eq. (1) because the force F was not projected to the normal direction, and therefore misses the factor $(R_{out} \cos\theta - R_{in})/d$ inside the integration. For small inter-wall spacing $R_{out} - R_{in} = \sigma/2$ (not shown in Fig. 2), all pressures are positive (i.e., repulsive force), while they become negative (i.e., attractive force) for large inter-wall spacing $R_{out} - R_{in} = 2\sigma$. Figure 2 also shows the normalized product of pressure and radius, $pR/(8\pi\varepsilon\sigma^2\rho_c^2)$, which has different signs for the inner and outer walls, and therefore $p_{in} R_{in} \neq p_{out} R_{out}$.

There exist other potentials that are more accurate than the Lennard-Jones 6-12 potential to represent the C-C repulsive term, such as a registry dependent potential to describe the corrugation in interlayer interactions in graphene nanostructures (Kolmogorov $et\ al.$ [10]), or a modified Morse potential based on the ab initio LDA calculations (Wang $et\ al.$ [11]) that has been verified for graphite subject to high pressure[12]. We use the Morse-type potential[11] to calculate the pressures p_{in} and p_{out} of a double-wall CNT with an inner wall radius 0.35nm and the inter-wall spacing 0.3nm. The resulting pressures are p_{in}=35.0 and p_{out}=6.7GPa, which give $p_{in} \neq p_{out}$ and $p_{in} R_{in} \neq p_{out} R_{out}$. These conclusions also hold, in general, for other potentials.

Equations (1) and (2) are used to study buckling of a double-wall CNT subjected to external pressure p_{ext}. The deformation is uniform prior to buckling, but its rate becomes

non-uniform at the onset of buckling.   The analysis is similar to that for a single-wall CNT[13] except that

(i) the outer wall is subjected to a net external pressure p_{ext}-p_{out};

(ii) the inner wall is subjected to an external pressure p_{in}; and

(iii) p_{in} and p_{out} are related to the inner and outer wall radii R_{in} and R_{out} via Eqs. (1) and (2).

Figure 3 shows the critical external pressure at the onset of buckling, $(p_{ext})_{cr}$, versus L/R_{out} for a (8,8)@(13,13) double-wall CNT, where L and R_{out} are the length and outer radius; $(p_{ext})_{cr}$ is much larger than that for the outer wall [(13,13) single-wall CNT][13], almost 4 times for long CNTs. This reflects the resistance of vdW force between walls against buckling.   Results based on prior assumptions overestimate the critical external pressure for buckling; the assumption $p_{in} = p_{out}$ overestimates by 75% for long CNTs, and $p_{in}R_{in} = p_{out}R_{out}$ overestimates by 26%.
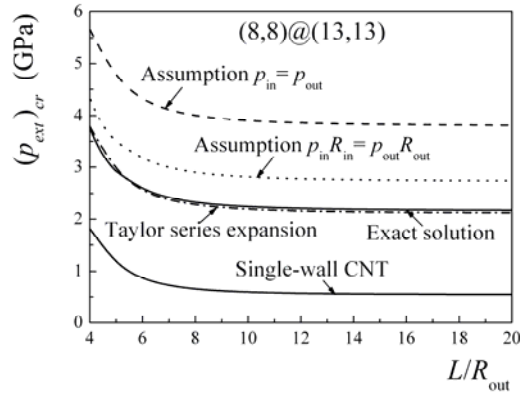

Figure 3.   The critical external pressure at the onset of buckling, $(p_{ext})_{cr}$, versus the length to outer radius ratio, L/R_{out}, for a (8,8)@(13,13) double-wall CNT.   Results for the (13,13) single-wall CNT, and those based on prior assumptions are also shown.

Equations (1) and (2) can be expressed in the Taylor series of the small parameter

$$\xi = \left(R_{out} - R_{in} \right)/\left(R_{out} + R_{in} \right) \quad \text{as}$$

$$p = -8\pi\varepsilon\sigma\rho_c^2 \left\{ \begin{array}{l} \left[\left(\dfrac{\sigma}{R_{out}-R_{in}}\right)^5 \left(1+\dfrac{1}{8}\xi^2\right) - \left(\dfrac{\sigma}{R_{out}-R_{in}}\right)^{11}\left(1+\dfrac{7}{20}\xi^2\right)\right] \\ \pm\dfrac{3}{4}\xi\left[\left(\dfrac{\sigma}{R_{out}-R_{in}}\right)^5 - \dfrac{6}{5}\left(\dfrac{\sigma}{R_{out}-R_{in}}\right)^{11}\right] + O\left(\xi^3\right) \end{array} \right\}, \qquad (3)$$

where + terms are for p_{in} and – terms for p_{out}. Similarly, $p_{in}R_{in}$ and $p_{out}R_{out}$ are given by

$$pR = -8\pi\varepsilon\sigma^2\rho_c^2 \left\{ \begin{array}{l} \left[\left(\dfrac{\sigma}{R_{out}-R_{in}}\right)^4 \left(\dfrac{1}{2\xi}-\dfrac{5}{16}\xi\right) - \left(\dfrac{\sigma}{R_{out}-R_{in}}\right)^{10}\left(\dfrac{1}{2\xi}-\dfrac{11}{40}\xi\right)\right] \\ \pm\left[-\dfrac{1}{8}\left(\dfrac{\sigma}{R_{out}-R_{in}}\right)^4 + \dfrac{1}{20}\left(\dfrac{\sigma}{R_{out}-R_{in}}\right)^{10}\right] + O\left(\xi^2\right) \end{array} \right\}, \qquad (4)$$

where + terms are for $p_{in}R_{in}$ and – terms for $p_{out}R_{out}$. For the inter-wall spacing $R_{out}-R_{in}=\sigma$

as in Fig. 2, $p_{in}, p_{out} = 0.6\pi\varepsilon\sigma\rho_c^2\left(\pm 2\xi + 3\xi^2\right)$ (and therefore $p_{in} \neq p_{out}$), and

$p_{in}R_{in}, p_{out}R_{out} = 0.3\pi\varepsilon\sigma^2\rho_c^2\left(\pm 2 + \xi\right)$ (and therefore $p_{in}R_{in} \neq p_{out}R_{out}$). Figure 3 also shows the

critical external pressure at the onset of buckling, $(p_{ext})_{cr}$, based on the Taylor series expansion (3)

and (4), which agrees very well with the exact solution based on Eqs. (1) and (2).

The last example to illustrate $p_{in} \neq p_{out}$ and $p_{in}R_{in} \neq p_{out}R_{out}$ is for two concentric tubes

with electrical charges, which are characterized by the electrostatic potential $V(d) \sim d^{-1}$ and

force $F = V'(d) \sim d^{-2}$, where $d = \sqrt{R_{in}^2 + R_{out}^2 - 2R_{in}R_{out}\cos\theta + z^2}$ is the distance between

electrical charges. The electrical charges on the inner and outer tubes are represented by their

area densities (number of charges per unit area) ρ_{in} and ρ_{out}. The pressures on the inner and

outer walls are then given by $p_{in} = \rho_{in}\rho_{out}R_{out}\int_{-\infty}^{\infty}dz\int_0^{2\pi} F\left(R_{out}\cos\theta - R_{in}\right)d^{-1}d\theta$ and

$p_{out} = \rho_{in}\rho_{out}R_{in}\int_{-\infty}^{\infty}dz\int_0^{2\pi} F\left(R_{out} - R_{in}\cos\theta\right)d^{-1}d\theta$. For $F = V'(d) \sim d^{-2}$, it can be shown

analytically that the pressure on the inner wall is identically zero, $p_{in} \equiv 0$, while the pressure on the outer wall is not, $p_{out} \neq 0$, such that $p_{in} \neq p_{out}$ and $p_{in}R_{in} \neq p_{out}R_{out}$.

In summary, continuum models for van der Waals force or electrostatic force between CNT walls are obtained analytically. They bypass assumptions in prior studies, and have been applied to determine the critical external pressure for buckling of double-wall CNTs.

[1]   B. I. Yakobson, C. J. Brabec, and J. Bernholc, Phys. Rev. Lett. **76** (14), 2511-2514 (1996).

[2]   Y. Huang, J. Wu, and K. C. Hwang, Phys. Rev. B **74** (24), 245413 (2006).

[3]   P. Zhang, Y. Huang, H. Gao, and K.C. Hwang, ASME J. Appl. Mech. **69** (4), 454-458 (2002).

[4]   J. Wu, K. C. Hwang, and Y. Huang, J. Mech. Phys. Solids **56** (1), 279-292 (2008).

[5]   L. A. Girifalco, M. Hodak, and R. S. Lee, Phys. Rev. B **62** (19), 13104-13110 (2000).

[6]   A. Pantano, D. M. Parks, and M. C. Boyce, J. Mech. Phys. Solids **52** (4), 789-821 (2004).

[7]   C. Q. Ru, J. Mech. Phys. Solids **49** (6), 1265-1279 (2001).

[8]   X. Q. He, S. Kitipornchai, and K. M. Liew, J. Mech. Phys. Solids **53** (2), 303-326 (2005).

[9]   W. B. Lu, J. Wu, L. Y. Jiang, Y. Huang, K.C. Hwang and B. Liu, Philo. Mag. **87** (14-15), 2221-2232 (2007).

[10]   A. K. Kolmogorov and V.H. Crespi, Phys. Rev. B **71**, 235415 (2005).

[11]   Y. Wang, D. Tomanek and G. F. Bertsch, Phys. Rev. B **44**, 6563-6565 (1991).

[12]   D. Qian, W. K. Liu and R. S. Ruoff, J. Phys. Chem. B **105**, 10753-10758 (2001).

[13]   J. Wu, K. C. Hwang, J. Song, and Y. Huang, ASME J. Appl. Mech. **75** (6), 061006 (2008).